Research Square

Preprints are preliminary reports that have not undergone peer review.
They should not be considered conclusive, used to inform clinical practice,
or referenced by the media as validated information.

Identification of Biomarkers for m6A-Mediated Programmed Cell Death in Osteoarthritis Transcripts with Experimental Validation.

Gang Xue
Xi'an Daxing Hospital
Yihai Liu
3497932251yh@163.com

Affiliated Hospital of Gansu Medical College

Article

Keywords:

Posted Date: April 9th, 2026

DOI: https://doi.org/10.21203/rs.3.rs-9134544/v1

License: This work is licensed under a Creative Commons Attribution 4.0 International License.
Read Full License

Additional Declarations: No competing interests reported.

Identification of Biomarkers for m6A-Mediated Programmed Cell Death in Osteoarthritis Transcripts with Experimental Validation.

Gang Xue [1] ; Yihai Liu [2] *.

[1] Department of Orthopedics,Xi'an Daxing Hospital, Xi'an ,710003 China.

[2] Department of Orthopedics, Affiliated Hospital of Gansu Medical College, Ping'liang 744000, China.

*Corresponding author:

Yihai Liu, E-mail: 349793225lyh@163.com.

Abstract

Introduction: Osteoarthritis (OA) is a common progressive joint disorder with limited treatment options. Emerging evidence suggests that N6-methyladenosine (m6A)-mediated programmed cell death (PCD) plays a crucial role in OA progression, yet the key regulatory genes remain unidentified. This study aims to identify m6A-modified PCD biomarkers to facilitate improved OA management.

Materials and Methods: We performed a comprehensive multi-omics analysis using transcriptomic data from two independent OA cohorts. Differentially expressed genes were integrated with 1,548 PCD-related genes and 23 m6A regulators. Feature selection was conducted using LASSO regression and Boruta algorithm. Biomarkers were validated through cross-dataset consistency verification, ROC curve analysis, and RT-qPCR. Mechanistic insights were explored through gene set enrichment analysis, immune infiltration deconvolution, and drug-gene interaction prediction.

Results: Integration analysis identified 26 candidate genes, from which machine learning selected six key genes. Five biomarkers (TNFAIP3, MYC, CDKN1A, ATF3, and CX3CR1) were robustly validated. These genes are involved in inflammatory and apoptotic pathways. Immune infiltration analysis revealed increased M2 macrophages, resting mast cells, plasma cells, and Tregs in OA tissues. Cadmium compounds were predicted as potential therapeutics. RT-qPCR confirmed significant downregulation of TNFAIP3, MYC, CDKN1A, and ATF3 in OA patients.

Conclusions: This study identified five m6A-PCD-related biomarkers associated with OA pathogenesis, providing new insights into OA mechanisms and potential therapeutic targets.

1. Introduction

As a progressive musculoskeletal disorder, OA manifests through the chronic degradation of joint cartilage and adjacent subchondral bone structures.As the most prevalent cause of joint pain and mobility impairment in the elderly, OA significantly impacts quality of life and poses a growing global health burden. Epidemiological data indicate that over 30% of individuals above 60 years are affected, with OA-related healthcare expenditures accounting for 8-10% of total chronic disease costs. The disease

predominantly affects weight-bearing joints (hips, knees, ankles), often beginning with localized symptoms that may progress to involve adjacent joints. Characteristic pathological changes include cartilage erosion, synovial inflammation, and abnormal bone remodeling, ultimately leading to joint structural damage.

OA pathogenesis involves complex interactions between intrinsic biological factors and extrinsic environmental influences**Error! Reference source not found.**. Genetic predispositions, particularly mutations in IL-1 β and RUNX2 genes, contribute to dysregulated inflammatory responses and bone metabolism. These interact with mechanical stress, metabolic disorders, and lifestyle factors to initiate and accelerate disease progression**Error! Reference source not found.Error! Reference source not found.**. Current diagnostic approaches combine clinical assessment with imaging and histopatholo gical examination. However, early detection remains challenging due to initially subtle molecular changes preceding macroscopic damage. While existing treatments focus on symptom management and disease modification, they cannot reverse established pathology. Further research into synovial tissue mechanisms and early biomarkers is urgently needed to develop targeted therapies[4-[5].

1.1 Programmed Cell Death (PCD) and m6A Methylation in Osteoarthritis Pathogenesis

Programmed Cell Death (PCD) is an active, genetically regulated process essential for maintaining physiological homeostasis, tissue remodeling, and responding to pathological stimuli. Dysregulated PCD contributes to developmental disorders, cancers, and OA, where uncontrolled cell death exacerbates cartilage degradation and joint dysfunction. PCD encompasses multiple forms, including apoptosis (non-lytic) and pyroptosis (lytic, pro-inflammatory). In OA, osteoblast pyroptosis accelerates cartilage loss, while other PCD pathways (e.g., ferroptosis, necroptosis) further drive disease progression[6].

N6-methyladenosine (m6A), a dynamic RNA modification, regulates gene expression by influencing RNA stability, processing, and translation. It plays critical roles in cellular processes such as proliferation, survival, and PCD[7]. In OA, the m6A writer METTL3 exhibits dual roles: it promotes fibroblast-like synoviocyte senescence by suppressing autophagy-related genes, yet protects chondrocytes by stabilizing anti-apoptotic Bcl2 mRNA. The epitranscriptome, particularly m6A-modified long non-coding RNAs (lncRNAs), modulates OA pathogenesis through cartilage metabolism, inflammation, and PCD[8] .

1.2 Interplay Between PCD and m6A in OA:

Emerging evidence highlights a mechanistic link between m6A and PCD in OA. m6A dynamics regulate key bone metabolism pathways, where mRNA stabilization and signaling modulation jointly control cell survival or death. For instance, m6A-marked RNAs (e.g., OsQP1) may influence bone density by targeting downstream genes. This dual regulatory axis offers potential therapeutic targets for OA and related bone disorders[9].

This study accessed transcriptomic data from OA and normal synovial tissues via the GEO database to identify candidate genes linked to m6A modification and PCD. Using two machine learning algorithms, we pinpointed six genes as potential m6A-PCD-related biomarkers for OA. Their expression patterns were verified by qPCR. Further analyses included drug target prediction, immune cell infiltration assessment, functional enrichment, and regulatory network construction. These findings offer novel insights for OA diagnosis and therapeutic strategies[10].

2. Materials and Methods

2.1 Data Collection and Processing

Synovial tissue transcriptome datasets were acquired from the GEO public repository. For model development, we selected dataset GSE55235 (Affymetrix GPL96 platform) consisting of 10 OA-

affected and 10 healthy synovial samples. Independent dataset GSE12021 (same platform) with 9 control and 10 OA samples served for validation. The complete repertoire of 1,548 cell death-related genes was compiled from existing publication while 23 m6A regulatory genes were identified through comprehensive literature mining[12].

2.2 Preliminary Gene Screening

Transcriptome-wide expression differences were analyzed using the limma differential expression framework (version 3.50.1)[12]. Results were graphically represented through customized visualization tools: differentially expressed genes were plotted using ggplot2 (v3.4.4)**Error! Reference source not found.**, while expression patterns were displayed via ComplexHeatmap (v2.14)**Error! Reference source not found.**. Integration of m6A and PCD gene sets was performed through correlation network analysis (psych package v2.4.3)[13]applying stringent selection criteria (absolute correlation >0.6, *p*-value <0.05). The overlapping gene set from these analyses formed our initial candidate pool.

2.3 Biological Interpretation

Functional annotation of candidate genes was conducted through integrated pathway analysis using clusterProfiler (v4.7.1.3)[13]. Both Gene Ontology terms and KEGG pathways were examined with statistical significance determined at $p<0.05$.Biological interpretation was enhanced through advanced visualization techniques implemented in GOplot (v1.0.2)[14].

2.4 Interactome Mapping

Protein-protein interaction networks were constructed using STRING database with high-confidence interactions (score>0.7). Network visualization and analysis were performed in Cytoscape environment (v3.7.2)[17], with non-interacting nodes removed from further consideration.

2.5 Computational Feature Selection

Our analytical pipeline incorporated:1.Regularized regression modeling (LASSO via glmnet v4.1-6)[18] with five-fold cross-validation, where optimal regularization parameter (λ) was selected by minimum cross-validated error.2.Random forest-based feature importance analysis (Boruta v8.0.0)[19] retaining features with Z-score >2.3.The consensus gene set from both approaches was designated as key candidates.

2.6 Multi-cohort Validation

Expression patterns of key genes were examined across both datasets using non-parametric statistical testing (Wilcoxon rank-sum, $p<0.05$). Diagnostic potential was evaluated through receiver operating characteristic analysis (pROC v1.18)[20], considering AUC values >0.7 as demonstrating clinical utility. Only genes showing consistent expression patterns and diagnostic performance in both independent cohorts were advanced as final biomarkers.

2.7Systems-level Pathway Analysis

Genome-wide co-expression patterns were established for each biomarker. These signature profiles were subjected to gene set enrichment analysis using clusterProfiler (v4.7.1.3) against curated pathway collections (MSigDB c2.cp.v2023.2.Hs)[21], with significant pathways identified at $p<0.05$, false discovery rate <25%, and normalized enrichment score magnitude >1.

2.8Immunological Characterization

The compositional patterns of 22 distinct leukocyte subsets were analyzed using the CIBERSORT computational method integrated within the IOBR analytical toolkit (release 0.99.8)**Error! Reference source not found.**. Immune cell distribution profiles were statistically compared between osteoarthritis patients and healthy controls employing the Wilcoxon rank-sum test, with a

significance threshold set at $p<0.05$. Subsequent correlation assessments of significantly altered immune populations were conducted using Spearman's ρ coefficient, applying dual thresholds of $|\rho|>0.3$ and $p<0.05$ for meaningful associations. Systematic evaluation of biomarker-immunocyte relationships was performed, with exclusion of non-significant correlations ($p\geq0.05$) from graphical representations to enhance data interpretability.

2.9 Computational analysis of molecular interactions was conducted through multiple bioinformatics approaches. Protein interaction networks for the identified biomarkers were generated using GeneMANIA's web-based interface, which integrates diverse biological data sources. For regulatory element identification, putative miRNA binding sites were predicted through miRNet's algorithmically curated database, while transcription factor interactions were determined using experimentally validated ENCODE ChIP-seq datasets. These regulatory relationships were computationally integrated and graphically represented as a tripartite regulatory network using Cytoscape's visualization toolkit (v3.9.1). Concurrently, computational drug repositioning analysis was performed by interrogating the DSigDB compound database through the enrichR analytical pipeline (v3.1)[22], applying a significance threshold of FDR-adjusted p-value <0.05. The most statistically significant pharmacological agents (top 10 candidates) were incorporated into the network visualization to illustrate potential therapeutic associations.

2.10 Experimental Validation

Biomarker expression was validated in clinical samples using RT-qPCR. Five pairs of frozen tissue samples (OA synovium from patients with orthopedic synovitis/ligament injuries vs normal synovium) were obtained from Affiliated Hospital of Gansu Medical College under approved ethics protocol.(Samples were taken from patients with orthopedic synovitis and ligament injuries and normal synovial joints in Affiliated Hospital of Gansu Medical College. The study passed the hospital ethics audit. Ethics number ： 2025010.Total RNA was extracted from 50 mg tissue using TRIzol reagent (Ambion, USA) following the manufacturer's protocol: homogenization in 1 ml TRIzol, 10-min incubation on ice, addition of 300 μl chloroform, vigorous shaking, 10 min room temperature incubation, centrifugation at 12000g and 4° C for 15 min. The aqueous phase was mixed with an equal volume of ice-cold isopropyl alcohol (Chronchem, China), incubated at room temperature for 10 min, and centrifuged at 12000g and 4° C for 10 min. The RNA pellet was washed twice with 1 ml 75% ethanol (Chronchem, China) (centrifugation at 7500g, 4° C for 5 min), air-dried, and dissolved in RNase-free water (Servicebio, China). RNA concentration was measured using a NanoPhotometer N50 (Implen, Germany).

The complementary DNA was synthesized from messenger RNA utilizing the SureScript First-Strand cDNA Synthesis Kit (Servicebio, China) in a BIO-RAD thermal cycler under optimized reaction conditions comprising an initial incubation at 25° C for 5 minutes to facilitate primer annealing, followed by reverse transcriptionat 50° C for 15 minutes and enzyme deactivation at 85° C for 5 seconds, with a final temperature hold at 4° C for reaction stabilization. The synthesized cDNA products were subsequently diluted 5-20 fold using nuclease-free molecular biology grade water to achieve appropriate template concentrations（Table 3）. Quantitative polymerase chain reaction analysis was conducted on a CFX96 Real-Time PCR Detection System (BIO-RAD, USA)（Table 4）employing gene-specific primer pairs (Tsingke Biotechnology, China; detailed sequences available in Supplementary （Table 5）under carefully standardized cycling parameters: an initial denaturation step at 95° C for 60 seconds, followed by 40 cycles of denaturation at 95° C for 120 seconds, primer annealing at 55° C for 20 seconds, and extension at 72° C for 30 seconds. Post-amplification analysis included generation of

amplification curves and dissociation profiles, with automatic recording of cycle threshold values by the instrument's proprietary software for subsequent quantitative analysis of gene expression patterns.

Component	Volume
5x Reaction Buffer	4ul
Primer	1ul
SweScript RT I Enzyme Mix	1ul
Total RNA	2ug
Nuclease-Free Water	Add to 20ul

Table 3 reverse transcription reagent

Component	Volume
cDNA	3ul
2xUniversal Blue SYBR Green qPCR Master Mix	5ul
Forward primer (10μM)	1ul
Reverse primer (10μM)	1ul

Table 4 qPCR reaction system

Primer	Sequence
TNFAIP3 F	AGAGAGATCACACCCCCAGC
TNFAIP3 R	GTGCTCTCCAACACCTCTCC
MYC F	CCCTCCACTCGGAAGGACTA
MYC R	CGTTGTGTGTTCGCCTCTTG
CDKN1A F	TGCCGAAGTCAGTTCCTTGT
CDKN1A R	CATTAGCGCATCACAGTCGC
ATF3 F	CACAGCTCTCTTCTCTCGCC
ATF3 R	GGATGGCAAACCTCAGCTCT
CX3CR1 F	ACTGCTGGTGGACTTCTTCC
CX3CR1 R	CACAGTCCCAAAGACCACGA
Internal reference-GAPDH F	CGAAGGTGGAGTCAACGGATTT
Internal reference-GAPDH R	ATGGGTGGAATCATATTGGAAC

Table 5 Primer sequences

2.11 Statistical Analysis

All statistical analyses were performed using R software (V 4.2.3). A p-value < 0.05 was considered statistically significant.

3. Results

3.1 Identification of 159 DEGs, 525 PCD-m6A Genes, and 26 Candidate Genes

Analysis of the training set (GSE55235) identified 159 DEGs between OA and control groups (Figure 1A), comprising 85 upregulated genes (including IGH, IGHG1, IGVL1-44, etc.) and 74 downregulated genes (CYP4B1, FOSB, MAFF, etc.); their expression levels are shown in Figure 1B. Spearman correlation analysis identified 525 genes as significantly correlated with both PCD and m6A regulators (PCD-m6A genes; Supplementary Table 1). Intersection of DEGs and PCD-m6A genes yielded 26 candidate genes (Figure 1C).

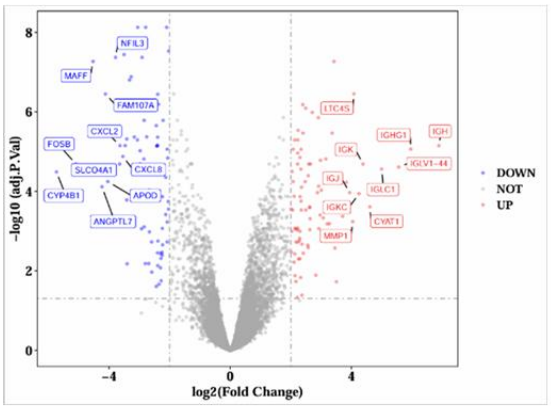


Fig.1A

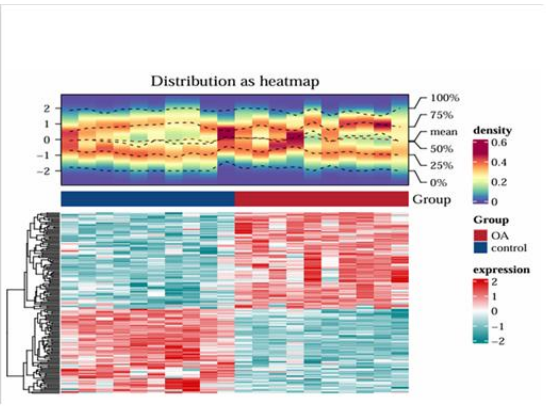


Fig.1B

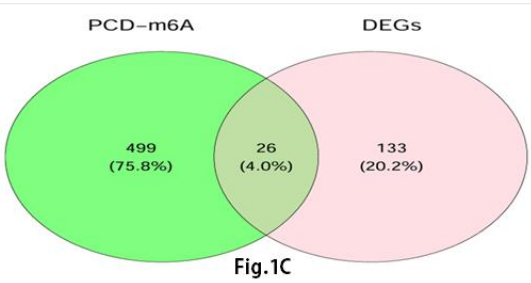


Fig.1C

3.2 Functional Enrichment: 1097 GO Terms, 70 KEGG Pathways, and PPI Network

Comprehensive GO analysis detected statistically significant enrichment in 1,097 functional terms (Supplementary Table 2), with the majority (1,019 terms) representing biological processes, followed by molecular functions (62 terms) and cellular components (16 terms).Figure 2A shows the number of up- and down-regulated genes in the top 5 significantly enriched pathways for BPs, MFs, and CCs. Key enriched GO terms included regulation of apoptotic signaling pathway (BPs), organelle outer membrane (CCs), and cytokine receptor binding (MFs). KEGG enrichment identified 70 significant pathways (Figure 2B), including Hepatitis B, IL-17 signaling pathway, and rheumatoid arthritis (RA), suggesting potential shared mechanisms between OA and RA. Using the STRING database (interaction score >0.7), we generated a protein-protein interaction network from 26 candidate genes, yielding 17 interconnected genes with 34 interactions after removing 9 non-interacting genes (Figure 2C). The most prominent network hubs included JUN, CXCL8, IL6, MMP9, and PTGS2.

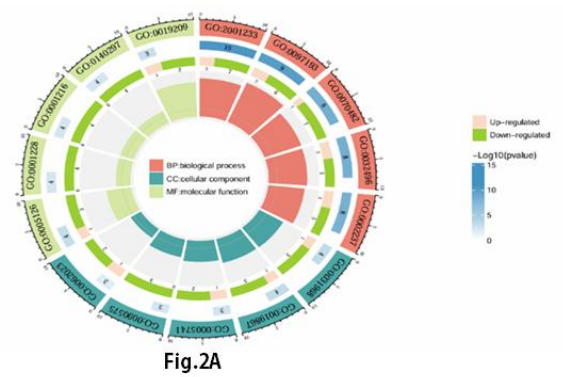


Fig.2A

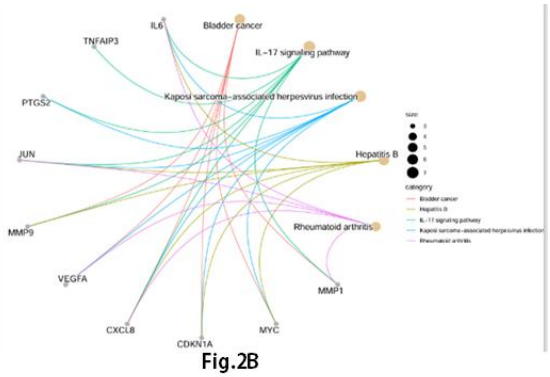


Fig.2B

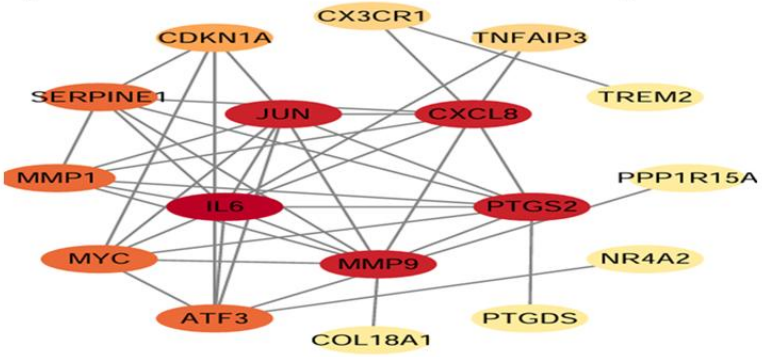


Fig.2C

3.3Machine Learning-Based Discovery of Six Core Genetic Markers

Two machine learning methods were applied to the 17 genes in the PPI network. LASSO regression (log(lambda min) = -5.4068) identified 6 key genes (Figure 3A, B). Boruta feature selection identified 16 genes with importance scores > 2 (Figure 3C). Intersection of genes selected by both methods yielded six key genes: TNFAIP3, MYC, CDKN1A, ATF3, MMP9, and CX3CR1 (Figure 3D).

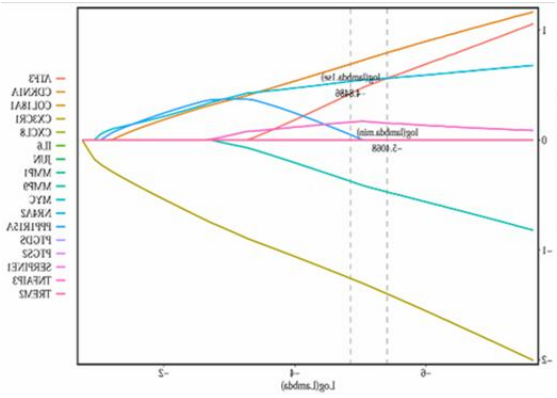


Fig.3A

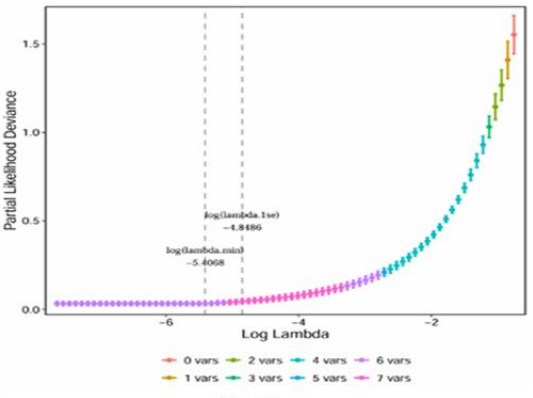


Fig.3B

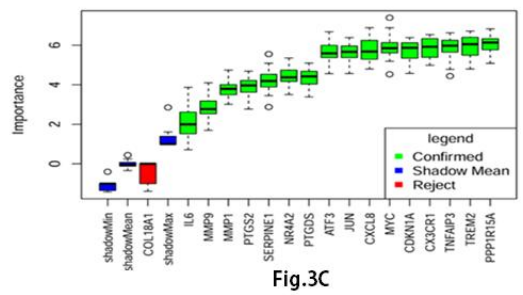


Fig.3C

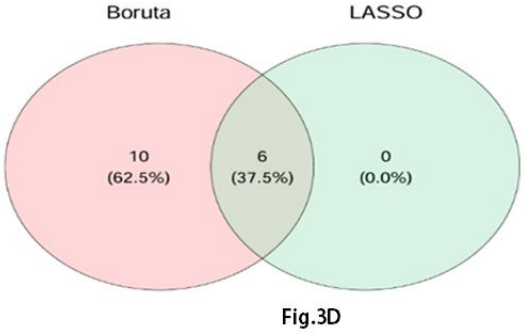


Fig.3D

3.4 Validation and Identification of Five OA Biomarkers

Quantitative assessment confirmed that all six genes exhibited significant expression differences in the training dataset (Figure 4A): CX3CR1 and MMP9 were upregulated in OA, while TNFAIP3, MYC, CDKN1A, and ATF3 were downregulated. In the validation set, MMP9 did not show significant differential expression (Figure 4B) and was excluded. ROC analysis demonstrated excellent diagnostic accuracy (AUC > 0.8) for the remaining five genes (TNFAIP3, MYC, CDKN1A, ATF3, CX3CR1) in both datasets (Figure 4C, D), confirming their status as biomarkers.

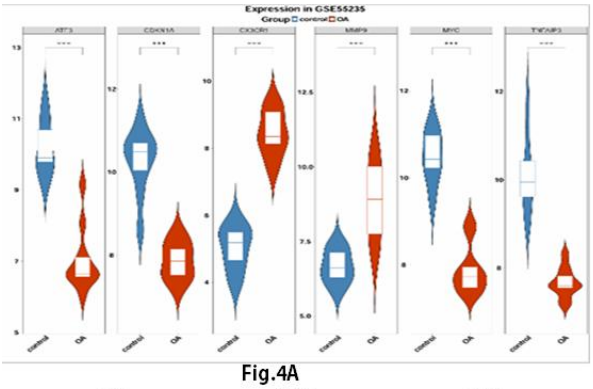


Fig.4A

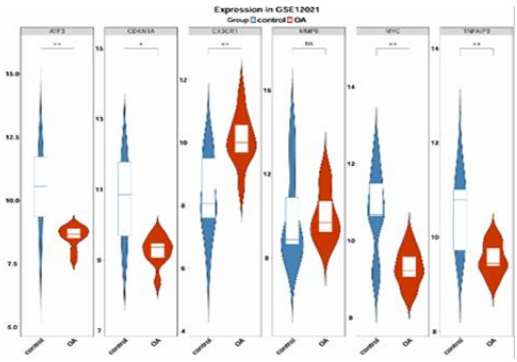


Fig.4B

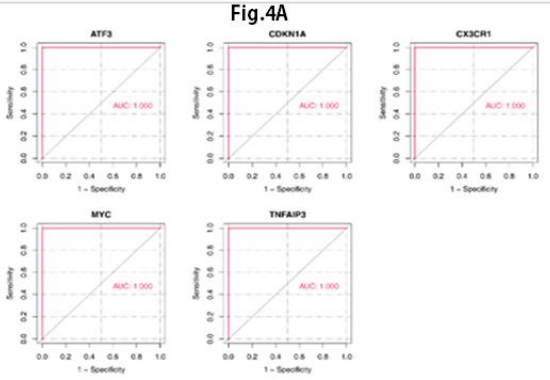


Fig.4C

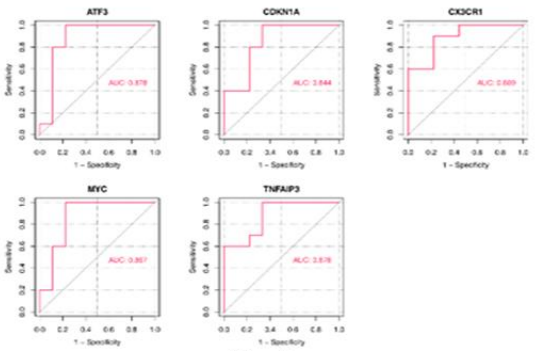


Fig.4D

3.5 GSEA Results

GSEA was performed for each of the five biomarkers, with the top 5 enriched pathways visualized per biomarker (Figure 5A-E). ATF3 was enriched in 246 pathways (e.g., lysosome, neutrophil degranulation, glucocorticoid receptor pathway). CDKN1A was enriched in 216 pathways (e.g., lysosome, C-MYC active, response to metal ions). CX3CR1 was enriched in 181 pathways (e.g., spliceosome, mRNA processing, glucocorticoid receptor pathway). MYC was enriched in 245 pathways (e.g., spliceosome, mRNA processing, RNA splicing). TNFAIP3 was enriched in 201 pathways (e.g., lysosome, RNA processing, glucocorticoid receptor pathway). Notably, the glucocorticoid receptor pathway was enriched by all five biomarkers. This pathway was upregulated in ATF3, CDKN1A, MYC, and TNFAIP3, but downregulated in CX3CR1, suggesting its crucial role in OA pathology and potential treatment response.

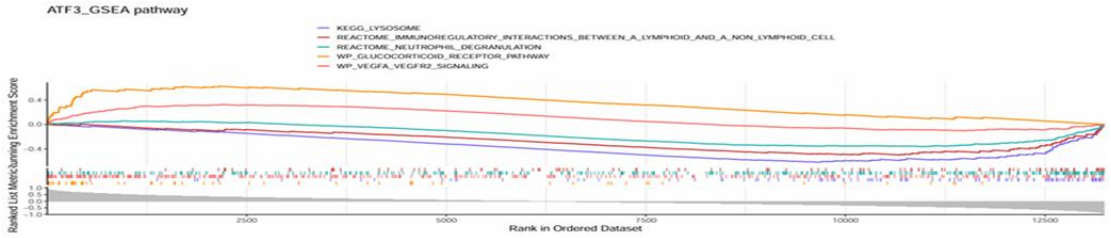


Fig.5A

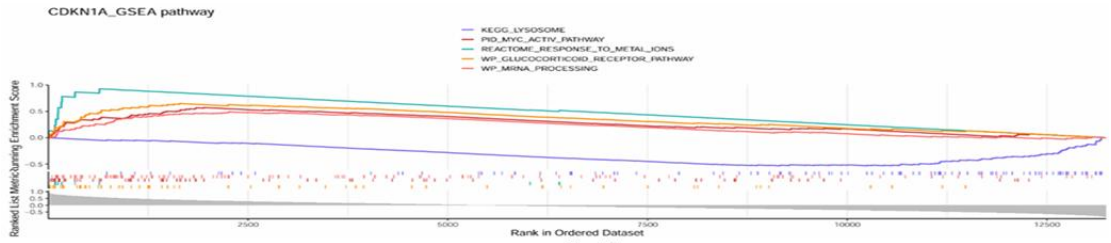


Fig.5B

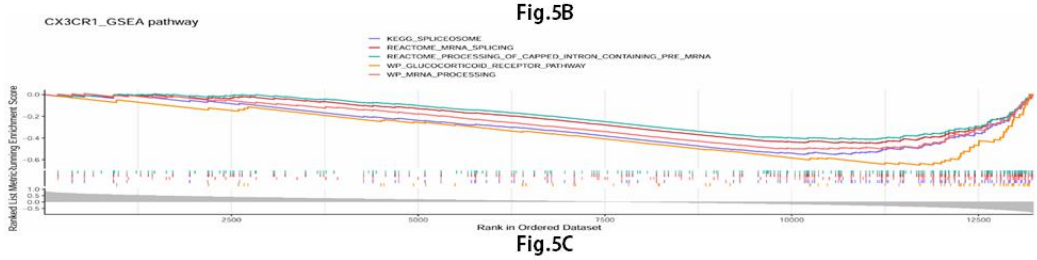


Fig.5C

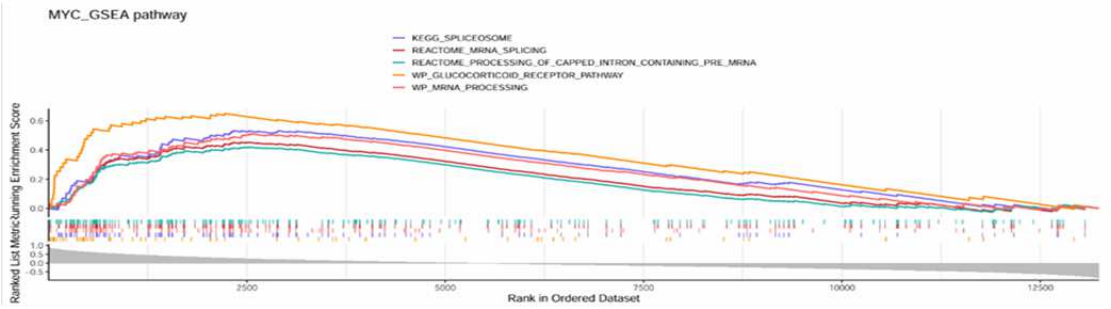


Fig.5D

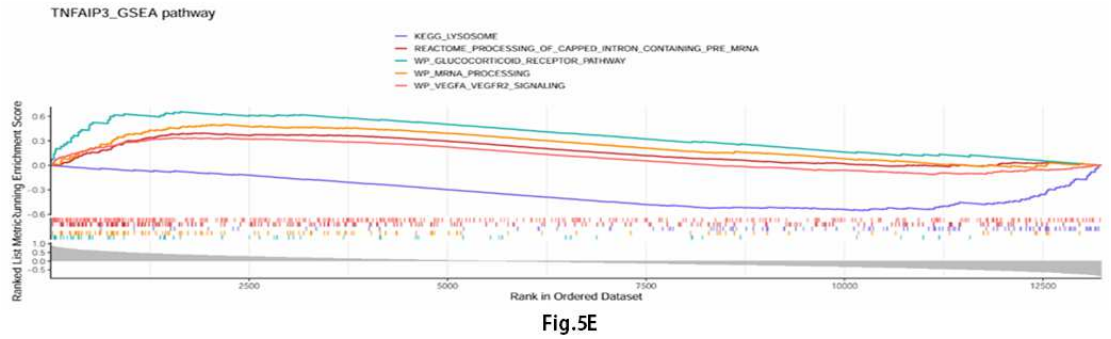


Fig.5E

3.6 Immune Infiltration Differences, Inter-Immune Cell Correlations, and Biomarker Links

Immune infiltration analysis revealed M2 macrophages as the most abundant immune cell type in both groups (Figure 6A). Significantly higher infiltration levels of M2 macrophages, resting mast cells, plasma cells, and regulatory T cells (Tregs) were observed in OA compared to controls. Comparative immune cell analysis demonstrated distinct distribution patterns between groups, with control samples exhibiting increased frequencies of activated mast cells and resting CD4+ memory T cells. Differential infiltration

analysis identified six immune cell subsets with significant abundance variations (Figure 6B). Examination of intercellular relationships revealed four positively associated immune cell pairs (including M2 macrophages and resting mast cells) and ten negatively correlated pairs (such as resting CD4+ memory T cells and resting mast cells) (Figure 6C). Biomarker-immune cell correlation mapping showed ATF3 expression inversely related to M2 macrophages, resting mast cells, and plasma cells, while displaying positive associations with resting CD4+ memory T cells and activated mast cells. Complete correlation profiles for other biomarkers are presented in (Figure 6D).

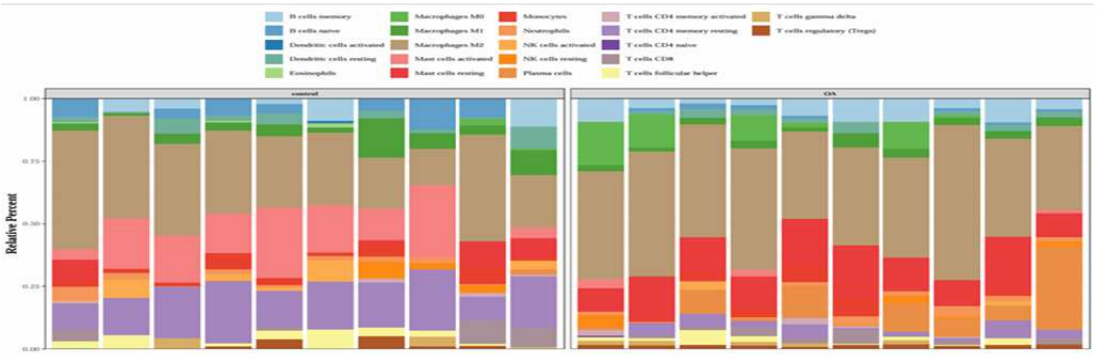


Fig.6A

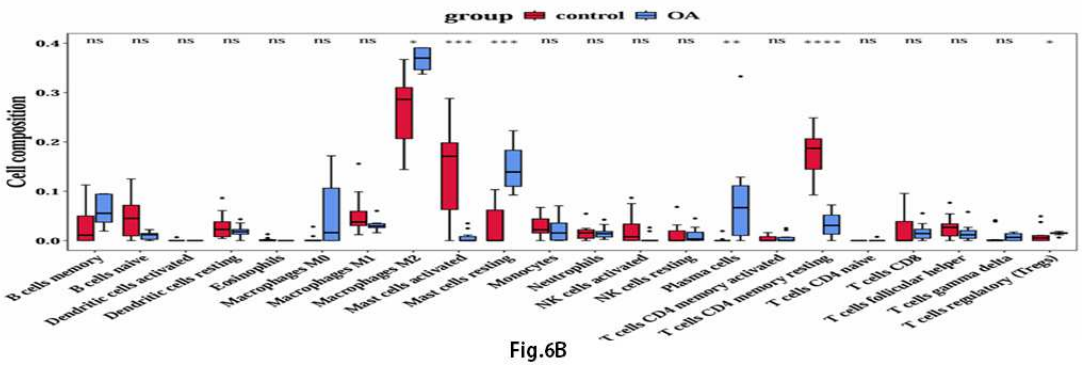


Fig.6B

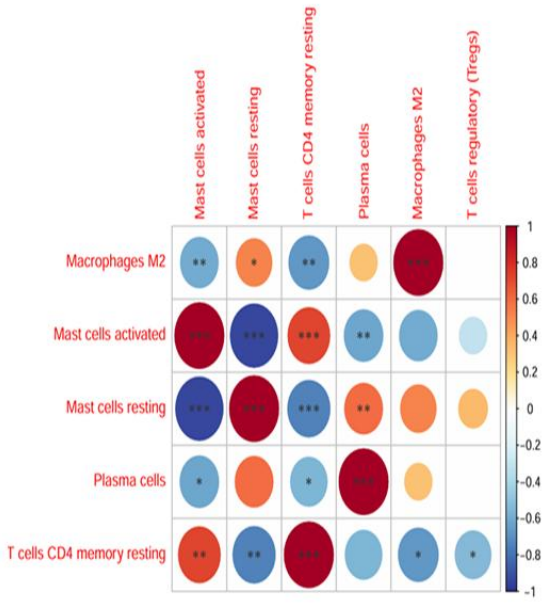


Fig.6C

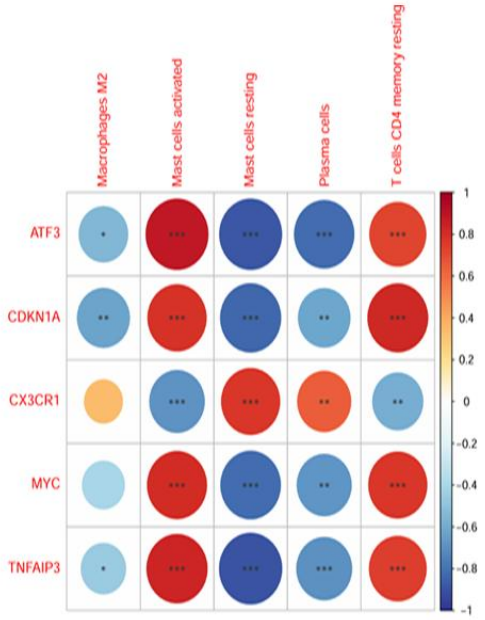


Fig.6D

3.7 Construction of Three Networks for the Five Biomarkers

The GGI network for the five biomarkers, constructed using GeneMANIA, involved 20 interacting genes (Figure 7A). Physical interactions constituted the largest proportion (77.64%), followed by co-expression (8.01%). Bioinformatic interrogation of the gene network uncovered three core functional modules:1.Cell cycle control apparatus(1)G1/S checkpoint governance;(2)CDK activation dynamics;(3)Cyclin docking mechanisms;2.Kinase modulation network:(1)Serine/threonine phosphorylation cascades;(2)Kinase activity fine-tuning(3)Signal transduction fidelity;3.Structural orchestration:(1)Kinase complex stoichiometry(2)Spatial-temporal organization(3)Macromolecular assembly.miRNA prediction identified 1,385 unique miRNAs targeting the biomarkers (ATF3: 157, CDKN1A: 922, CX3CR1: 31, MYC: 493, TNFAIP3: 361). TF prediction identified 206 unique TFs (ATF3: 39, CDKN1A: 105, CX3CR1: 9, MYC: 62, TNFAIP3: 104). The regulatory network visualized 9 miRNAs targeting all five biomarkers and 19 TFs targeting at least three biomarkers (33 nodes, 105 edges; Figure 7B). The drug-biomarker interaction network (15 nodes, 30 edges; Figure 7C) visualized the top 10 predicted drugs; CADMIUM was predicted to target all five biomarkers.

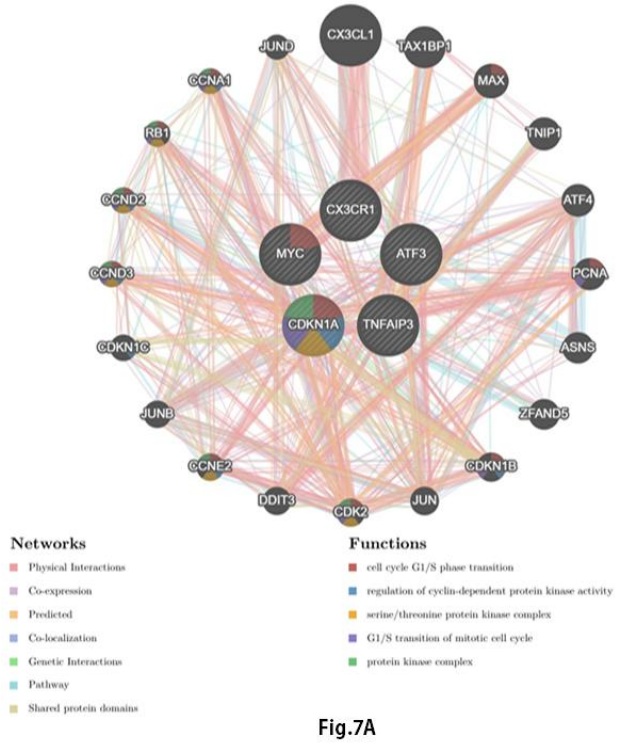


Fig.7A

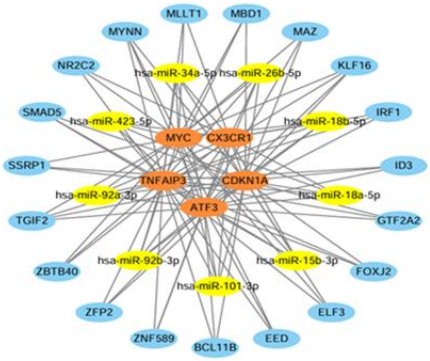


Fig.7B

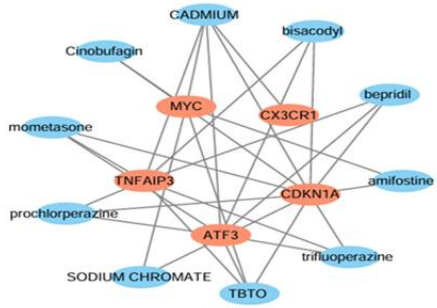
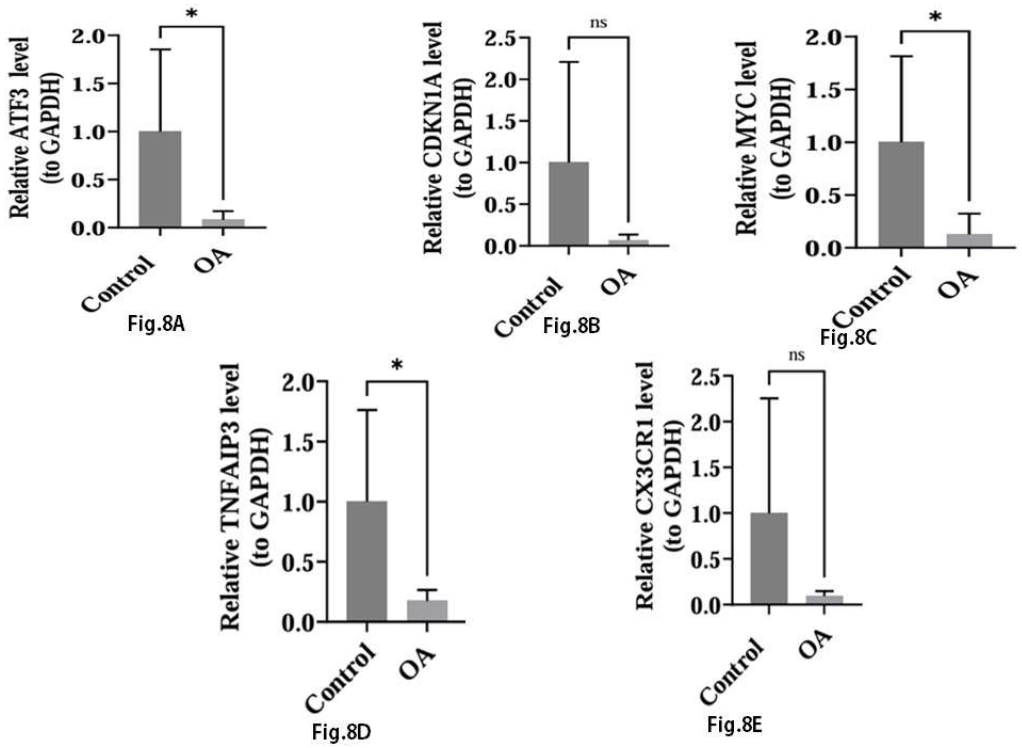


Fig.7C

3.8 RT-qPCR Validation Results

Molecular validation through RT-qPCR revealed three key findings: (1) The mRNA expression of TNFAIP3, MYC, CDKN1A, and ATF3 was significantly downregulated in OA patient samples versus healthy controls ($p<0.05$, Figures 8A-D); (2) While CX3CR1 expression showed a similar decreasing trend, it failed to achieve statistical significance ($p>0.05$, Figure 8E); (3) The observed expression patterns of TNFAIP3, MYC, CDKN1A, and ATF3 showed remarkable congruence with our bioinformatics predictions. This multi-level verification strongly corroborates the validity of our analytical pipeline and findings.



4. Discussion

As a common degenerative joint condition, OA progressively damages cartilage, causing persistent pain, joint stiffness, and impaired physical function. Research in recent years has demonstrated that programmed cell death (PCD) is a pivotal regulatory mechanism in OA progression, acting as an essential intermediary linking multifactorial contributors to cartilage pathological injury[24]. PCD, a genetically regulated process, encompasses various forms including apoptosis, necroptosis, and ferroptosis, each contributing to cartilage homeostasis and pathology. However, the precise molecular mechanisms by which different PCD forms interact to drive OA progression remain incompletely understood, limiting the development of targeted therapeutic strategies[25]-[27]. This study systematically evaluated the contributions of various PCD forms to OA pathogenesis and their underlying signaling pathways through bioinformatics analysis and experimental validation. By clarifying how dysregulated PCD (e.g., aberrant chondrocyte death) accelerates cartilage breakdown, we further explored potential therapeutic interventions targeting these PCD-related pathways. Our findings highlight the significance of PCD modulation in OA management and provide a theoretical basis for translating mechanistic insights into effective clinical therapies.

We identified and validated five key biomarker genes: TNFAIP3, MYC, CDKN1A, ATF3, and CX3CR1. TNFAIP3 (A20) is a critical negative regulator of inflammatory signaling pathwa ys, particularly TNF-induced NF-κB activation. Articular cartilage stem cells (ACSCs) exert pr otective effects in OA partly through secreting TNFAIP3. Its downregulation in OA (RT-qPCR validated) likely compromises this anti-inflammatory protection, exacerbating synovitis and cartil age degradation**Error! Reference source not found.**.

MYC, a conserved regulator of proliferation and stress responses, was downregulated in OA patients. GSEA indicated MYC enrichment in the glucocorticoid receptor (GR) pathway, crucial for OA chondroprotection and anti-inflammation[29]. MYC downregulation may therefore impair GR-mediated anti-inflammatory responses.MYC also participates in spliceosome/mRNA processing pathways, suggesting potential cooperation with m6A modification in regulating stress-response genes. Regulatory network analysis identified hsa-miR-34a-5p as a likely MYC-targeting miRNA, suggesting a post-transcriptional downregulation mechanism. Given MYC's core role in proliferation and inflammation, functional interplay with TNFAIP3 (an NF-κB inhibitor) is plausible: MYC downregulation may alleviate NF-κB suppression, worsening OA inflammation. Targeting MYC or its regulators represents a potential OA therapeutic strategy[31].

CDKN1A (p21), a cell cycle inhibitor regulating G1/S transition and proliferation-apoptosis balance, was significantly downregulated in OA. This likely reflects perturbed stress responses, where impaired proliferation prevents essential cell cycle arrest needed for repair, exacerbating matrix degradation[32]. GSEA revealed enrichment in GR and lysosomal pathways. Downregulation may thus weaken GR-mediated anti-inflammation and, via NF-κB crosstalk, amplify inflammation (e.g., promoting MMP-13 activation). It may also impair senescent cell clearance, accelerating degeneration. Co-enrichment with ATF3/TNFAIP3 in the GR pathway suggests synergistic dysregulation exacerbates OA pathology. CDKN1A downregulation is a key marker of chondrocyte dysfunction.

ATF3, a stress-responsive transcription factor crucial for chondrocyte protection under chronic stress, was significantly downregulated in OA. This disruption weakens its suppressive effect on the NF-κB/MAPK signaling pathways, leading to excessive production of pro-inflammatory cytokines such as interleukin-6 (IL-6) and tumor necrosis factor-alpha (TNF-α)[33]. Consequently, synovial inflammation is aggravated, which aligns with the observed elevation in pro-inflammatory immune cell infiltration. GSEA showed ATF3 enrichment in the anti-inflammatory GR pathway. Its downregulation likely attenuates GR activation, synergistically amplifying inflammation alongside reduced TNFAIP3/CDKN1A. ATF3 downregulation compromises dual protection against inflammation and stress.

CX3CR1, a chemokine receptor mediating immune cell migration and inflammation, was downregulated in OA (though RT-qPCR did not reach significance). This may influence OA progression via: (1) Immune Dysregulation: Impairing macrophage regulation, potentially promoting M1 polarization and pro-inflammatory cytokine/MMP secretion[34]. (2) Pathway Disruption: Enrichment in spliceosome/GR pathways suggests downregulation could disrupt NF-κB balance (causing hyperactivation) and weaken GR anti-inflammation[35]. (3) Altered Cellular Crosstalk: Impairing interactions with M2 macrophages/resting mast cells, disrupting recruitment balance. CX3CR1 downregulation represents a key OA pathological marker[36].

Collectively, the differential expression of these five genes is closely associated with core OA pathological mechanisms: TNFAIP3 and ATF3 likely exert chondroprotective effects by suppressing excessive inflammation and stress-induced damage, while CDKN1A and MYC may regulate cell cycle progression to maintain chondrocyte metabolic and proliferative balance. The role of CX3CR1 appears complex, potentially promoting inflammatory cell infiltration that exacerbates cartilage degradation. These findings highlight their critical, interconnected roles in OA pathogenesis.

Gene set enrichment analysis (GSEA) demonstrated that all five biomarkers were significa ntly associated with the glucocorticoid receptor signaling pathway. Additionally, these biomarker s were implicated in other biological processes, including lysosomal function, spliceosome activ ity, and mRNA processing. This aligns with the central role of m6A modification in RNA pro cessing and translational regulation. Notably, the GR pathway was upregulated in ATF3, CDK N1A, MYC, and TNFAIP3 but downregulated in CX3CR1, suggesting this pathway contributes to the balance between inflammatory responses and chondrocyte survival in OA through coordi nated regulation by different biomarkers. This finding echoes the known mechanism of glucoco rticoids in OA clinical treatment, where they exert anti-inflammatory effects and inhibit cartilag e degradation.

Regulatory network analysis identified key regulatory nodes: Nine microRNAs (including h sa-miR-34a-5p and hsa-miR-101-3p) and nineteen transcription factors (such as SMAD5 and IR F1) were identified as regulators targeting these biomarkers.miR-34a-5p influences cell proliferat ion and apoptosis by targeting MYC family genes, while SMAD5, a key TGF-β signaling mo lecule, may regulate CDKN1A to participate in chondrocyte cycle arrest. These TF-miRNA-bio marker interaction networks illustrate how m6A modification may synergistically influence PCD -related gene expression in OA through epigenetic and post-transcriptional regulation, providing a multi-layered perspective on OA molecular mechanisms.

Taken together, these results validate the essential role of programmed cell death in drivin g OA progression, with the identified regulatory mechanisms revealing potential opportunities f or therapeutic development. Specifically,RIPK1/RIPK3-mediated necroptosis and NLRP3 inflamm asome activation signaling pathways show promise as potential drug targets. Future research sh ould elucidate the precise molecular mechanisms of these pathways to design therapies capable of precisely modulating PCD in OA, potentially improving cartilage degeneration beyond sympt om alleviation.

Limitations: This study utilized public databases, potentially introducing heterogeneity affec ting interpretation. Although preliminary validation established an association between m6A mo dification and OA biomarkers, its exact mechanistic role requires further experimental verificati on. Subsequent studies should focus on: (1) clarifying the regulatory details of PCD-related pat hways involving these biomarkers; and (2) deciphering the specific molecular mechanisms of m 6A modification in regulating these genes in OA, validated with larger clinical cohorts to facili tate biomarker-based drug development.

Although these limitations exist, our research offers fresh perspectives on the molecular un derpinnings of osteoarthritis (OA) and establishes a foundation for developing targeted therapeut ic approaches.Our subsequent work will follow research advances concerning these genetic fact ors and examine their pathogenic significance in OA. The discovery of this m6A-PCD regulato ry axis opens new avenues for targeted therapies in degenerative joint diseases.

Declarations

Data availability statement: The datasets analysed during the current study are available in the [Gene Expression Omnibus] repository, [GSE55235: https://ww w.ncbi.nlm.nih.gov/geo/query/acc.cgi?acc=GSE55235 and GSE12021: https://www. ncbi.nlm.nih.gov/geo/query/acc.cgi?acc=GSE12021]

Conflict of Interest： This research did not receive any specific grant from funding agencies in the public, commercial, or not-for-profit sectors.

Author Contribution： G.X: Conceptualization, Data curation, Validation, Visualization, Writing – original draft, Writing – review & editing. YH.L: Visualization, Writing – review & editing. XX: Conceptualization, Supervision, Writing – review & editing. T.J: Conceptualization, Project administration, Supervision, Writing – review & editing. This work currently described has not been published, is not being considered for publication elsewhere, and its publication was approved by all authors.

Ethics approval and consent to participat: This study was performed in line with the principles of the Declaration of Helsinki and approved by the Ethics Committee of the Ethics Committee of the Affiliated Hospital of Gansu Medical College. The approval number of approval are as follows: 2025010. All patients provided written informed consent at the time of clinical sample collection for experiments, ensuring that the research process complied with ethical norms and that patients' rights and wishes were fully respected.

Funding： This research received no specific grant from funding agencies in the public, commercial, or not-for-profit sectors.

5.Reference

[1] Englund M. (2023). Osteoarthritis, part of life or a curable disease? A bird's-eye view. Jo urnal of internal medicine 293:681–693. https://doi.org/10.1111/joim.13634

[2] Hunter, D. J., & Bierma-Zeinstra, S. (2019). Osteoarthritis. Lancet (London, England).393: 1745–1759. https://doi.org/10.1016/S0140-6736(19)30417-9

[3] Horváth, E., Sólyom, Á., Székely, J., Nagy, E. E., & Popoviciu, H. (2023). Inflammatory and Metabolic Signaling Interfaces of the Hypertrophic and Senescent Chondrocyte Phenot ypes Associated with Osteoarthritis. International journal of molecular sciences.24:164-168. https://doi.org/10.3390/ijms242216468

[4] Tang, Y., Wang, Z., Cao, J., & Tu, Y. (2025). Bone-brain crosstalk in osteoarthritis: path ophysiology and interventions. Trends in molecular medicine.31:281–295. https://doi.org/10. 1016/j.molmed.2024.09.006

[5] Abramoff, B., & Caldera, F. E. (2020). Osteoarthritis: Pathology, Diagnosis, and Treatmen t Options. The Medical clinics of North America.104:293–311. https://doi.org/10.1016/j.mcn a.2019.10.007

[6] Yuan, J., & Ofengeim, D. (2024). A guide to cell death pathways. Nature reviews. Molec ular cell biology.25:379–395. https://doi.org/10.1038/s41580-023-00689-6

[7] Zhai, G., Xiao, L., Jiang, C., Yue, S., Zhang, M., Zheng, J., Liu, Z., & Dong, Y. (2022). Regulatory Role of N6-Methyladenosine (m6A) Modification in Osteoarthritis. Frontiers in cell and developmental biology.10:946219. https://doi.org/10.3389/fcell.2022.946219

[8] Tang, Y., Hong, F., Ding, S., Yang, J., Zhang, M., Ma, Y., Zheng, Q., Yang, D., Jin, Y., & Ma, C. (2023). METTL3-mediated m6A modification of IGFBP7-OT promotes osteoarthritis progression by regulating the DNMT1/DNMT3a-IGFBP7 axis. Cell reports.42:112589. https://doi.org/10.1016/j.celrep.2023.112589

[9] Okuyan, H. M., & Begen, M. A. (2022). LncRNAs in Osteoarthritis. Clinica chimica acta; international journal of clinical chemistry.532:145–163. https://doi.org/10.1016/j.cca.2022.05.030

[10] Huang, M., Guo, J., Liu, L., Jin, H., Chen, X., & Zou, J. (2023). m6A demethylase FTO and osteoporosis: potential therapeutic interventions. Frontiers in cell and developmental biology.11:1275475. https://doi.org/10.3389/fcell.2023.1275475

[11] Qin, H., Abulaiti, A., Maimaiti, A., Abulaiti, Z., Fan, G., Aili, Y., Ji, W., Wang, Z., & Wang, Y. (2023). Integrated machine learning survival framework develops a prognostic model based on inter-crosstalk definition of mitochondrial function and cell death patterns in a large multicenter cohort for lower-grade glioma. Journal of translational medicine.21:588. https://doi.org/10.1186/s12967-023-04468-x

[12] Ritchie, M. E., Phipson, B., Wu, D., Hu, Y., Law, C. W., Shi, W., & Smyth, G. K. (2015). limma powers differential expression analyses for RNA-sequencing and microarray studies. Nucleic acids research.43:e47. https://doi.org/10.1093/nar/gkv007

[13] Wu, T., Hu, E., Xu, S., Chen, M., Guo, P., Dai, Z., Feng, T., Zhou, L., Tang, W., Zhan, L., Fu, X., Liu, S., Bo, X., & Yu, G. (2021). clusterProfiler 4.0: A universal enrichment tool for interpreting omics data. Innovation (Cambridge (Mass.)).2:100141. https://doi.org/10.1016/j.xinn.2021.100141

[14] Gu Z. (2022). Complex heatmap visualization. iMeta.1:e43. https://doi.org/10.1002/imt2.43

[15] Robles-Jimenez, L. E., Aranda-Aguirre, E., Castelan-Ortega, O. A., Shettino-Bermudez, B. S., Ortiz-Salinas, R., Miranda, M., Li, X., Angeles-Hernandez, J. C., Vargas-Bello-Pérez, E., & Gonzalez-Ronquillo, M. (2021). Worldwide Traceability of Antibiotic Residues from Livestock in Wastewater and Soil: A Systematic Review. Animals : an open access journal from MDPI.12:60. https://doi.org/10.3390/ani12010060

[16] Walter, W., Sánchez-Cabo, F., & Ricote, M. (2015). GOplot: an R package for visually c ombining expression data with functional analysis. Bioinformatics (Oxford, England).31: 29 12–2914. https://doi.org/10.1093/bioinformatics/btv300

[17] Shannon, P., Markiel, A., Ozier, O., Baliga, N. S., Wang, J. T., Ramage, D., Amin, N., Schwikowski, B., & Ideker, T. (2003). Cytoscape: a software environment for integrated models of biomolecular interaction networks. Genome research.13:2498–2504. https://doi.org /10.1101/gr.1239303

[18] Friedman, J., Hastie, T., & Tibshirani, R. (2010). Regularization Paths for Generalized Lin ear Models via Coordinate Descent. Journal of statistical software.33:1–22.

[19] Yue, S., Li, S., Huang, X., Liu, J., Hou, X., Zhao, Y., Niu, D., Wang, Y., Tan, W., & Wu, J. (2022). Machine learning for the prediction of acute kidney injury in patients with sepsis. Journal of translational medicine.20:215. https://doi.org/10.1186/s12967-022-03364-0

[20] Robin, X., Turck, N., Hainard, A., Tiberti, N., Lisacek, F., Sanchez, J. C., & Müller, M. (2011). pROC: an open-source package for R and S+ to analyze and compare ROC curve s. BMC bioinformatics.12:77. https://doi.org/10.1186/1471-2105-12-77

[21] Xu, S., Hu, E., Cai, Y., Xie, Z., Luo, X., Zhan, L., Tang, W., Wang, Q., Liu, B., Wang, R., Xie, W., Wu, T., Xie, L., & Yu, G. (2024). Using clusterProfiler to characterize mul tiomics data. Nature protocols. 19:3292–3320. https://doi.org/10.1038/s41596-024-01020-z

[22] Zeng, D., Fang, Y., Qiu, W., Luo, P., Wang, S., Shen, R., Gu, W., Huang, X., Mao, Q., Wang, G., Lai, Y., Rong, G., Xu, X., Shi, M., Wu, Z., Yu, G., & Liao, W. (2024). En hancing immuno-oncology investigations through multidimensional decoding of tumor micr oenvironment with IOBR 2.0. Cell reports methods. 4:100910. https://doi.org/10.1016/j.crme th.2024.100910

[23] Zhang, L., Zhang, X., Guan, M., Zeng, J., Yu, F., & Lai, F. (2024). Machine-learning de veloped an iron, copper, and sulfur-metabolism associated signature predicts lung adenocar cinoma prognosis and therapy response. Respiratory research.25:206. https://doi.org/10.1186/ s12931-024-02839-6

[24] Kopeina, G. S., & Zhivotovsky, B. (2022). Programmed cell death: Past, present and futur e. Biochemical and biophysical research communications.633:55–58. https://doi.org/10.1016/ j.bbrc.2022.09.022

[25] Liu, S., Pan, Y., Li, T., Zou, M., Liu, W., Li, Q., Wan, H., Peng, J., & Hao, L. (2023). The Role of Regulated Programmed Cell Death in Osteoarthritis: From Pathogenesis to Th

erapy. International journal of molecular sciences.24:5364. https://doi.org/10.3390/ijms24065364

[26] Hwang, H. S., & Kim, H. A. (2015). Chondrocyte Apoptosis in the Pathogenesis of Osteoarthritis. International journal of molecular sciences.16:26035–26054. https://doi.org/10.3390/ijms161125943

[27] Ji, P., Zhou, Z., Zhang, J., Bai, T., Li, C., Zhou, B., Wang, M., Tan, Y., & Wang, S. (2024). Non-apoptotic cell death in osteoarthritis: Recent advances and future. Biomedicine & pharmacotherapy = Biomedecine & pharmacotherapie.179:117344. https://doi.org/10.1016/j.biopha.2024.117344

[28] Culver-Cochran, A. E., Hassan, A., Hueneman, K., Choi, K., Ma, A., VanCauwenbergh, B., O'Brien, E., Wunderlich, M., Perentesis, J. P., & Starczynowski, D. T. (2024). Chemotherapy resistance in acute myeloid leukemia is mediated by A20 suppression of spontaneous necroptosis. Nature communications.15:9189. https://doi.org/10.1038/s41467-024-53629-z

[29] Li, Z. L., Li, X. T., Hao, R. C., Wang, F. Y., Wang, Y. X., Zhao, Z. D., Li, P. L., Yin, B. F., Mao, N., Ding, L., & Zhu, H. (2023). Human osteoarthritic articular cartilage stem cells suppress osteoclasts and improve subchondral bone remodeling in experimental knee osteoarthritis partially by releasing TNFAIP3. Stem cell research & therapy.14:253. https://doi.org/10.1186/s13287-023-03411-7

[30] Rong, G., Zhang, Z., Zhan, W., Chen, M., Ruan, J., & Shen, C. (2025). VEGFA, MYC, and JUN are abnormally elevated in the synovial tissue of patients with advanced osteoarthritis. Scientific reports.15:2066. https://doi.org/10.1038/s41598-024-80551-7

[31] Li, X. T., Li, Z. L., Li, P. L., Wang, F. Y., Zhang, X. Y., Wang, Y. X., Zhao, Z. D., Yin, B. F., Hao, R. C., Mao, N., Xia, W. R., Ding, L., & Zhu, H. (2024). TNFAIP3 Derived from Skeletal Stem Cells Alleviated Rat Osteoarthritis by Inhibiting the Necroptosis of Subchondral Osteoblasts. Stem cells (Dayton, Ohio). 42:360–373. https://doi.org/10.1093/stmcls/sxad097

[32] Lan, Z., Yang, Y., Sun, R., Lin, X., Yan, J., Chen, X., Tian, K., Wu, G., Saad, M., Wu, Z., Xue, D., & Jin, Q. (2024). Characterization of PANoptosis-related genes with immunoregulatory features in osteoarthritis. International immunopharmacology.140:112889. https://doi.org/10.1016/j.intimp.2024.112889

[33] Tang, Y., Zhuo, D., Yu, Y., Pu, W., Ma, Y., Zhang, Y., Huang, Y., Zhang, Q., Tang, K., Meng, C., Yang, D., Bai, L., He, D., Jin, L., Zou, H., Xu, H., Zhu, Q., Wang, J., C

hen, Y., & Liu, J. (2024). Single-cell RNA sequencing reveals the CRTAC1+ population actively contributes to the pathogenesis of spinal ligament degeneration by SPP1+ macrophage. Aging cell, 23(12), e14320. https://doi.org/10.1111/acel.14320

[34] Gerlach, C., Moseman, E. A., Loughhead, S. M., Alvarez, D., Zwijnenburg, A. J., Waanders, L., Garg, R., de la Torre, J. C., & von Andrian, U. H. (2016). The Chemokine Receptor CX3CR1 Defines Three Antigen-Experienced CD8 T Cell Subsets with Distinct Roles in Immune Surveillance and Homeostasis. Immunity.45:1270–1284.

[35] Liu, X., Li, G., Yang, L., Pan, N., Tang, S., Yu, C., Zhang, Q., Zeng, L., Goswami, A., Deng, K., Liao, X., Tian, Y., & Wu, Y. (2025). Circular RNA PVT1 promotes osteoarthritis progression through the miR-550a-3p/CX3CR1 pathway: A mechanistic study. International immunopharmacology.163:115272. Advance online publication. https://doi.org/10.1016/j.intimp.2025.115272

[36] Ren, X., Manzanares, L. D., Piccolo, E. B., Urbanczyk, J. M., Sullivan, D. P., Yalom, L. K., Bui, T. M., Lantz, C., Najem, H., Dulai, P. S., Heimberger, A. B., Thorp, E. B., & Sumagin, R. (2023). Macrophage-endothelial cell crosstalk orchestrates neutrophil recruitment in inflamed mucosa. The Journal of clinical investigation.133:e170733. https://doi.org/10.1172/JCI170733